ESTIMATING AIR FLOW RATES IN A FUEL CELL SYSTEM USING ELECTROCHEMICAL IMPEDANCE

Judith O'Rourke and Murat Arcak
Department of Electrical Computer and Systems Engineering
Rensselaer Polytechnic Institute
Troy, NY 12180
orourj@rpi.edu and arcakm@rpi.edu

Manikandan Ramani
Plug Power Inc.
Latham, New York 12110
Manikandan_Ramani@plugpower.com

ABSTRACT

This paper proposes the use of electrochemical impedance spectroscopy (EIS) to estimate the cathode flow rate in a fuel cell system. Through experimental testing of an eight-cell, hydrogen-fueled polymer electrolyte stack, it shows that the ac impedance measurements are highly sensitive to the air flow rates at varying current densities. The ac impedance magnitude at 0.1Hz allows the distinction of air flow rates (stoichiometry of 1.5-3.0) at current densities as low as 0.1A/cm^2. Using experimental data and regression analysis, a simple algebraic equation that estimates the air flow rate using impedance measurements at a frequency of 0.1Hz is developed. The derivation of this equation is based on the operating cell voltage equation that accounts for all the irreversibilities.

INTRODUCTION

Over the past few decades fuel cell systems have gained a great deal of attention in the power industry. Production of electrical power using a fuel cell system is both environmentally friendly and efficient. As with all commercialization of products, huge efforts are made to reduce costs while improving and maintaining reliable efficient systems.

Electrochemical impedance spectroscopy (EIS) has proven to be a valuable tool in characterizing the electrical and mechanical properties of individual fuel cells or stacks. It has been used to evaluate the losses in individual PEM fuel cells [1], to diagnose a fuel cell stack with varying temperature, flow rates and humidity [2], to model a fuel cell as a transmission line circuit in order to characterize catalyst layer physics [3], and to detect dehydration and flooding [4]. As outlined in a US patent by Gasda et al. [5], impedance measurements can be taken with minimum cost to the system by adding appropriate circuitry to the power conditioning module.

The general pattern, shape and size of the Nyquist plots, reflecting impedance measurements taken over a spectrum of frequencies, have been the topic of many research papers. The impedance spectrum displays a high frequency loop and a low frequency loop. The low frequency loop is determined by the air mass-transfer in the GDL (gas diffusion layer) of the cathode [6]. As the cathode stoichiometry is reduced the low-frequency loop of the Nyquist plot enlarges [4].

This paper uses impedance measurements to estimate the air flow rate into the cathode thus eliminating the necessity of a flow meter. Flow meters are expensive and need to be frequently calibrated. Systems that do not use flow measurements must be run at higher than needed air flow rates to avoid the possibility of oxygen starvation that might lead to voltage reversal that will cause damage to the membrane [7]. Using impedance as a means of flow measurement would allow the system to run at lower air flows, thus reducing power to the compressor/blower and decreasing parasitic losses to the system. When used as a feedback signal, it would also improve system performance and account for manufacturing variability.

Our analysis shows that impedance measurements are sensitive to the flow rate of air into the cathode, and the degree of sensitivity is a function of the operating current density and the frequency at which the impedance is measured. As we discuss in Section 3.2, measuring impedance at a frequency of 0.1Hz allows the distinction between air flow rates (stoichiometry of 1.5 to 3.0) for current densities 0.1A/cm^2 and above. If impedance is measured at higher frequencies it becomes harder to discern between the lower air flow rates (0.4A/cm^2 and below.)

The proposed air flow estimation scheme consists of two steps: In Step 1, we use experimental data to obtain an expression for the limiting current density as a function of air flow. In Step 2, we use the theoretical equation for the operating cell voltage [8] to obtain an equation that relates impedance to limiting current density. Then, by combining equations obtained in Steps 1 and 2 we derive a formula that estimates the air flow from the impedance.

The rest of the paper is organized as follows: In Section 2, we discuss the experimental setup and instrumentation. In Section 3, impedance test results are presented, the limiting current density is modeled as a function of air flow and a statistical estimator of air flow rate is proposed. Section 4 gives the conclusions.

2. EXPERIMENTAL

Testing is performed in a laboratory at Plug Power Inc. in Latham, New York. The impedance experiments involve an eight cell stack with a 3M commercially available membrane electrode assembly. The membrane thickness is 1.1 mils (0.002794cm) and the active area of the cell is 262cm^2. The reactant flows to the stack are hydrogen and air. The anode and cathode gas streams are 100% humidified with external humidifiers. The coolant, air and hydrogen into the stack are heated with external heaters and the temperature of the gas into the cathode and anode are controlled to the same temperature as the coolant inlet temperature. During testing, the temperature for the coolant inlet is set to 55C.

National Instrument's SCXI and LabVIEW provide the user interface, signal processing and data logging. A HC Power Inc. load bank supplies the current load to the stack. The ac impedance testing is performed with a Solartron 1260A frequency response analyzer. To create the ac perturbation which is imposed on the dc bias, Solartron 1260A generates a signal that is inputted to an Encore (Model 619M-002) differential amplifier. The Encore conditions the input from the Solartron by adjusting the signal gain and filtering the amplifier output. The output from the differential amplifier is supplied to the (HC Power Inc.) load bank (slave) control input.

The voltage is measured across the entire stack and inputted to another Encore differential amplifier where the signal gain is adjusted and sent to input #1 of the Solartron. Sensed current (from the LEM current sensor) is inputted to the third Encore differential amplifier and then to input#2 on the Solartron. These amplifiers adjust signal outputs so that the Solartron receives signals that are in its operating range, 0-3Volts. Figure 1 summarizes the equipment used in impedance testing. A personal computer running the application, Zplot for Windows, is used to communicate with the Solartron through a GPIB interface board and to perform Electrochemical Impedance Spectroscopy measurements.

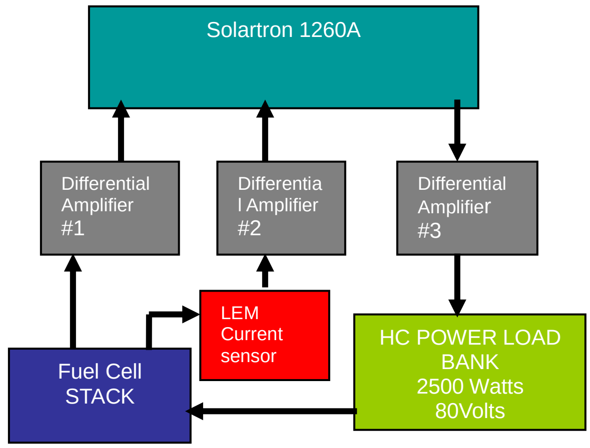

FIGURE 1. SCHEMATIC OF INSTRUMENTATION USED TO MEASURE IMPEDANCE OF A FUEL CELL STACK. DIFFERENTIAL AMPLIFIERS ARE USED TO AMPLIFY SIGNALS TO THE FREQUENCY RESPONSE ANALYZER.

Impedance measurements are taken in one of two ways: Operating conditions, reactant flows, load and temperatures are kept constant while the imposed ac signal (less than 5% of dc load) will vary in frequency from 0.1Hz to 15000Hz referred to as a "frequency sweep". The other method is to keep the frequency of the imposed signal constant and vary operating conditions.

3. RESULTS AND DISCUSSION

3.1 General Pattern of Impedance Sweeps

In this section we show that the air flow significantly affects the impedance spectrum at low frequencies. Three impedance sweeps are taken across an 8-cell module. The current density is kept constant at 0.7A/cm^2, inlet temperatures are constant at 55C and anode stoichiometry is fixed at 1.5. Figure 2 displays the sweeps at three different cathode stoichiometry; 1.5, 2.0 and 2.5. At frequencies of 150Hz to 15000Hz there is no change in the real and imaginary part of the impedance measurements; however at lower frequencies both the real and imaginary values significantly differ. At frequencies greater than 150Hz the change in impedance magnitude is less than 1%. At a frequency of 3Hz changing the cathode stoichiometry from 2.0 to 1.5 will increase the magnitude by 10% while increasing the cathode stoichiometry from 2.0 to 2.5 will decrease the magnitude by 6%. At a frequency of 0.1Hz the changes become +57% and -16% respectively.

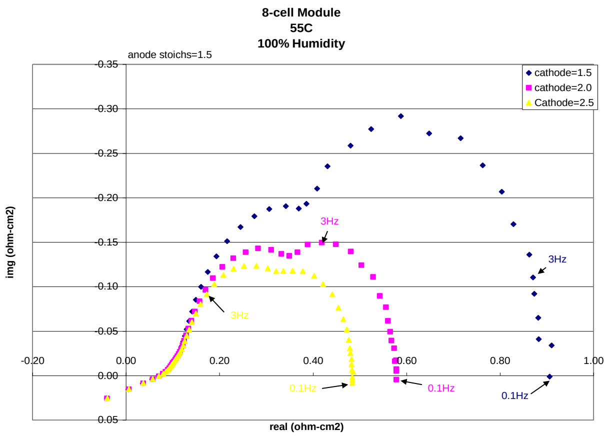

FIGURE 2. IMPEDANCE SWEEPS 0.1HZ TO 15,000HZ, CURRENT DENSITY AT 0.7A/CM^2 HYDROGEN IS HELD AT A CONSTANT FLOW RATE OF 15.4SLM AND AS THE AIR FLOW DECREASES FROM 60.9 TO 48.7 AND TO 36.5SLM BOTH THE REAL AND IMAGINARY PARTS OF IMPEDANCE INCREASE AT LOWER FREQUENCIES.

We next demonstrate that, unlike cathode flow rate, the hydrogen flow rate into the anode has little effect on the impedance measurements. The cathode flow rate is kept constant at a stoichiometry of 2.5 while the anode stoichiometry is varied. Figure 3 demonstrates that there is minimal change to the real or imaginary part of the measurements with anode stoichiometry varying from 1.5 to 1.9 to 2.0.

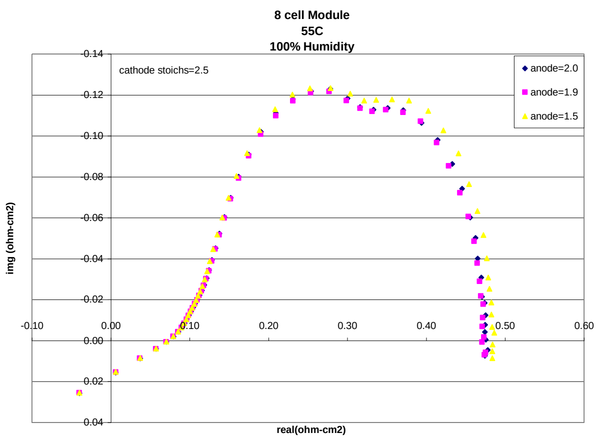

FIGURE 3. IMPEDANCE SWEEPS 0.1HZ TO 15,000HZ, CURRENT DENSITY AT 0.7A/CM^2, AIR IS HELD AT A CONSTANT FLOW RATE OF 60.9SLM AND THE HYDROGEN FLOW DECREASES FROM 20.5 TO 19.4 TO 15.4SLM. NO CHANGE IN IMPEDANCE MEASUREMENTS.

3.2 Impedance Measurements at a Constant Frequency

In the proposed estimation scheme, instead of a time consuming impedance frequency sweep, we would like to choose a single frequency which is sensitive to the air flow. The objective is to find a frequency that is fast enough not to disrupt the fuel cell system during operational mode but slow enough to be sensitive to air flow. Initially a frequency of 3Hz is selected because, as shown in Fig. 2, at 3Hz the impedance magnitude varied from 6% to 10%, with varying cathode flow rates. However, we show that this frequency is sensitive only to higher flow rates and is not appropriate for lower flow rates. We then show that the slower frequency of 0.1Hz is able to discern lower flow rates.

During the first test the frequency is held constant at 3Hz and eight step changes are made to the air flow rate (cathode stoichs of 1.5, 1.7, 1.9, 2.1, 2.3, 2.5, 2.7 and 3.0). At each flow rate, 70-75 impedance measurements are recorded. The hydrogen flow is kept at a constant stoichiometry of 1.9 to avoid any confounding effects due to anode flooding. In a real system, it is imperative to understand and separate anode and cathode flooding. However while characterizing the air flow dependence; the anode flow being constant eliminates any potential interaction.

The Zplot program used with the Solartron Analyzer is set to average 10 points before recording each impedance value. The dc load applied to the stack is at current density of 0.7A/cm^2. The humidity of reactant gases is 100% and the temperature of inlet flows is controlled to 55C. Figure 4 displays the Bode magnitude and phase plots. A clear distinction can be seen at each of the cathode flow rates.

It may appear that air flow can also be distinguished by voltage measurements. However, as shown in Fig. 4a the total voltage across the 8 cell module at each given air flow rate is not easily distinguishable. The voltage measurements displayed in Fig. 4a is the total voltage across the 8 cells during the impedance testing, so the voltage is following the 5% perturbation in the load signal. The mean voltage at the lowest air flow rate (1.5 stoichiometry) to the highest (3.0 stoichiometry) increases 5%, where the impedance magnitude changes 17%. The magnitude change is higher for impedance; in addition impedance response is in discrete amount when step changes are made in the flow rates.

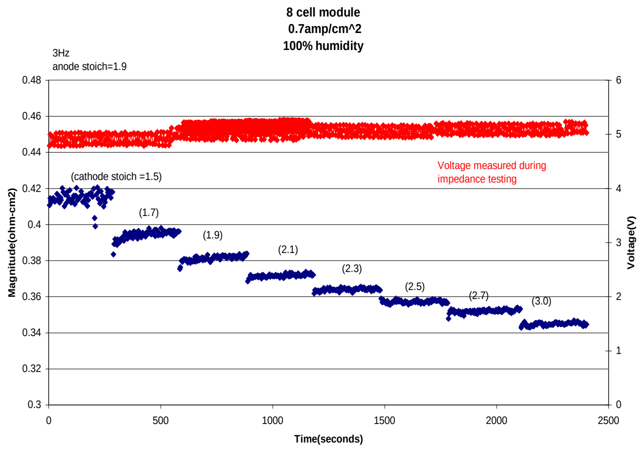

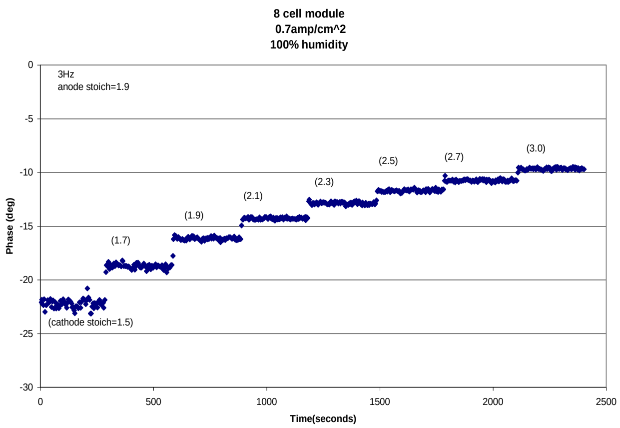

FIGURES 4A AND 4B. IMPEDANCE MAGNITUDE AND PHASE MEASURED AT 3HZ. DIFFERENT AIR FLOWS HAVE DISTINGUISHABLE IMPEDANCE MAGNITUDE AND PHASE VALUES AT OPERATING CONDITIONS FOR A CURRENT DENSITY OF 0.7A/CM^2, WHILE MEASURED VOLTAGE SHOWS LITTLE CHANGE.

The envisioned operating range for the application is 0.1A/cm^2 to 0.7A/cm^2. Though the results are encouraging at a current density of 0.7A/cm^2 a clear distinction must be achievable at the midrange and the lowest air flow rates. Figure 5 displays the results, at a current density of 0.4A/cm^2 and measured impedance at both 3Hz and 0.1Hz. The impedance measurements at 3Hz do not significantly vary at each step change in the air flow rate. The overall change in impedance magnitude and phase from an air flow rate of 20.88slm (1.5 stoichiometry) to 41.76slm (3.0 stoichiometry) is less than 5%. At the lower air flow rates corresponding to the lower current densities no distinction between impedance measurements can be made at 3Hz.

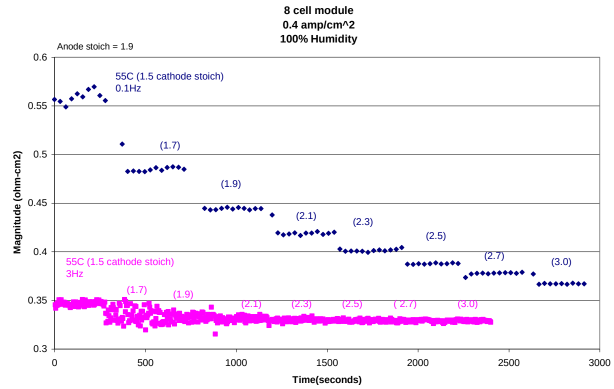

FIGURE 5. IMPEDANCE MAGNITUDE AND PHASE MEASURED AT 3HZ AND 0.1HZ, DIFFERENT AIR FLOWS HAVE DISTINGUISHABLE IMPEDANCE MAGNITUDE VALUES AT 0.1HZ BUT NOT AT 3HZ.

The test is then repeated at 0.1Hz with a slight revision. The test runs ten points at each of the eight air flow rates. Again the inlet flow temperatures are controlled to 55C, hydrogen and air are 100% humidified and anode stoichiometry is 1.9. The magnitude of impedance is clearly distinguishable for each change in cathode air flow. The change in voltage measurements during this test are insignificant. The total voltage at an air flow of 1.5 stoichiometry to an air flow of 3.0, increases from 5.7V to 5.8V (+1.7%). Most of this increase occurs from a stoichiometry of 1.5 to 1.7. Above 2.0 stoichiometry, the change in total voltage is less than 0.5%, smaller than the accuracy of the measurements.

The impedance testing was repeated at the lowest current density of 0.1A/cm^2 and, as expected, measuring the impedance magnitude at 3Hz did not distinguish between air flow rates, while at 0.1Hz there was a clear distinction. The magnitude of impedance measured at 0.1Hz varied from 1.0 ohm-cm^2 (at 1.5 stoichiometry) to 0.70 (at 3.0 stoichiometry) a 30% overall change, with at least a 4% change in each air flow step change.

3.3 Numerical Estimation of Air Flow Rate

Equation (1) below is used to determine the operating voltage for a fuel cell that accounts for ohmic losses, activation losses and concentration losses [8]:

$$V = E_o - R_\Omega i - \frac{RT}{\propto_c F} ln\left(\frac{C_o}{i_0}\right) - \frac{RT}{\propto_c F} ln\left(\frac{i}{\delta(i_l - i)}\right) \qquad (1)$$

E_o = open circuit potential (V)
R_Ω = ohmic resistance (ohm-cm^2)
i = current density (A/cm^2)
R = gas constant = 8.3145 (J/mol K)
F= Faraday's constant = 96485 (c/mol)
T= temperature (K)
α_c = oxygen reduction charge transfer factor
C_o = reference oxygen concentration (mol/cm^3)

i_o = exchange current density (A/cm^2)
δ = oxygen mass transfer coefficient (mol/A cm)
i_l = limiting current density (A/cm^2).

Since we focus on impedance measurements taken at the low frequency of 0.1Hz, the absolute value of the derivative of the DC voltage given in Eq. (1) will be a reasonable approximation for the impedance:

$$Z = R_\Omega + \frac{A}{i} + \frac{A}{(i_l - i)}$$
$$A = \frac{RT}{\alpha_c F} \qquad (2)$$

The dependence of the impedance Z in Eq. (2) on the air flow is through the limiting current density i_l. In a typical fuel cell, along with concentration distribution from inlet to outlet, current distribution also shows as much as two times at the inlet as compared to the outlet. The current distribution varies as a function of co-flow vs. counter flow. As the reactants are consumed, there is a concentration gradient that sets up across the GDL thickness resulting in maximum available current at the catalyst site given the mass-transport resistance across the thickness of the MEA. The reactants enter at a fixed concentration, but soon entering the reactor, starts off with gradient in the channel direction also, due to the consumption and water generation. Higher air flow rates minimize such gradients in the channel direction resulting in a more uniform current distribution from inlet to outlet. The true definition of a limiting current density is appreciated across the thickness of the package, whereas the maximum available current across the channel direction is fixed by the reactant flow and such a relationship can be established with air flow rates using an empirically related function generated by experiments as shown in Fig. 6.

The 8 cell module is tested at a constant current load and the air flow rate is reduced until the cell voltage drops to zero or one of the cells has negative voltage. The anode flow is held at a constant stoichiometry of 1.9. The test is repeated with increasing current loads. Figure 6 displays the results. Each set of points represents a fixed current density where the air flow is being slightly reduced till the voltage drops to zero or one or more cell voltages becomes negative. This defines the air flow rate that makes the fixed current density a limiting current density.

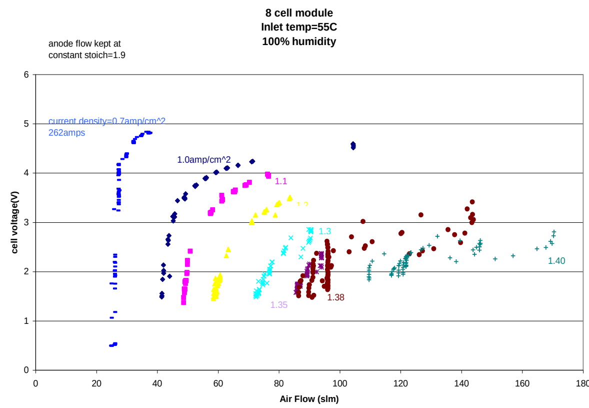

FIGURE 6. LIMITING CURRENT DENSITIES. EACH SET OF POINTS REPRESENTS A FIXED CURRENT DENSITY. THE AIR FLOW IS REDUCED TILL THE FIXED CURRENT DENSITY BECOMES THE LIMITING DENSITY. AS THE AIR FLOW INCREASES THE LIMITING CURRENT DENSITY INCREASES.

At each fixed current density the minimum air flow that can be achieved before voltage drops off is plotted in Fig. 7. Figure 7 demonstrates that as the air flow increases the limiting current density increases up to the structural limiting current density. To incorporate the effect of the structural limiting current density a natural logarithm is chosen for the curve fit:

$$i_l = 0.5405*\ln(\text{airflow}) - 1.0264. \qquad (3)$$

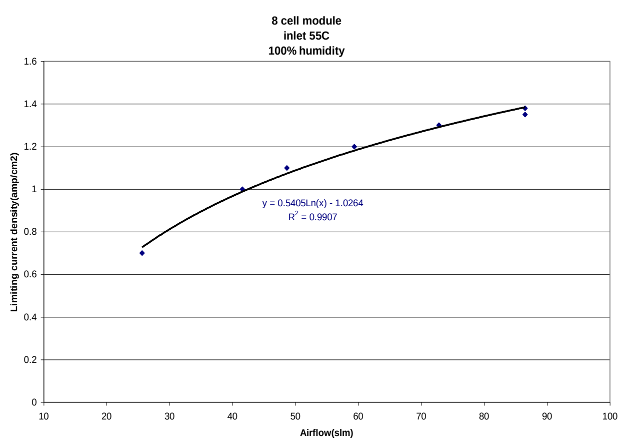

FIGURE 7. LIMITING CURRENT DENSITY VS. AIR FLOW. NATURAL LOG FIT TO ACCOUNT FOR THE STRUCTURAL LIMITING CURRENT DENSITY.

Outlined in Section 3.4 is the determination of R_Ω and A. Once these parameters are defined, Eq. (2) is manipulated to solve for the limiting current density and the limiting current density is replaced with the Eq. (3).

$$airflow(slm) = \exp\left(1.85\left(\frac{Zi - R_\Omega i}{Z - R_\Omega - \frac{A}{i}} + 1.0264\right)\right) \quad (4)$$

3.4 Determining Parameters R_Ω and A

The air flow estimate (Eq. 4) relies on the knowledge of R_Ω, and A. Parameter R_Ω, the ohmic resistance, can be experimentally measured and read from a Nyquist plot. Figure 8 displays the frequency sweeps (15,000 Hz to 0.1Hz) for current densities ranging from 0.1 to 0.7A/cm^2. The ohmic resistance is the impedance measurement at the high frequency where the curve crosses the real axis [2]. Note that for all current densities the curve crosses at a value approximately 0.10 ohm-cm^2.

To determine A (the Tafel slope) we use the impedance measurements in Fig. 8. We first determine the magnitude of the impedance at the lowest frequency for the lowest current density curve where mass transport losses are negligible. Following Eq. (2) we subtract R_Ω from this value and obtain the activation resistance which is equal to A divided by the current density. From Fig. 8 the 0.1A/cm^2 curve crosses the real axis (at the low frequency) at 0.7407 and results in A=0.064V.

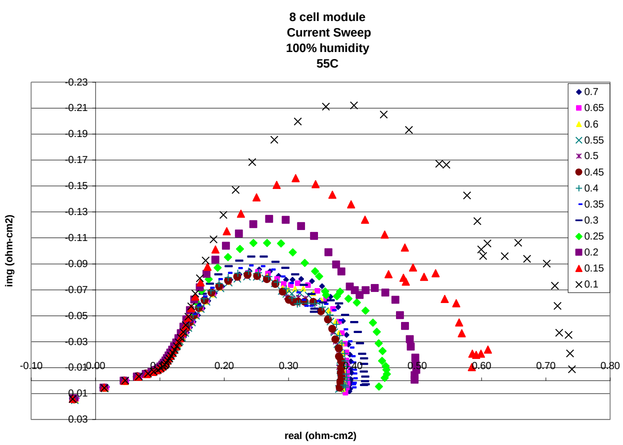

FIGURE 8. FREQUENCY SWEEPS FOR CURRENT DENSITIES VARYING FROM 0.1 TO 0.7A/CM^2. AT THE HIGH FREQUENCIES ALL THE CURRENT DENSITIES CROSS THE REAL AXIS AT 0.10OHM-CM^2. AT THE LOW FREQUENCY THE 0.1A/CM^2 CURVE CROSSES THE AXIS AT 0.7404OHM-CM^2.

Since real systems show degradation of catalyst, membrane and other fuel cell components, it is desirable to take impedance measurements at low current densities at high flows to eliminate mass-transport contribution. This value can be constantly updated, by taking discrete measurements in time on a pre-meditated fashion. It can be seen from Fig. 8, that while the impedance at 3 Hz seems to go down as current is increased, the dependence starts to reverse between 0.55 – 0.6 A/cm^2 . This indicates mass-transport signals start showing up at these current densities even at 3 Hz. As shown in Fig. 9, a plot of inverse current vs. impedance at 3 Hz from 0.1 to0.25 A/cm^2 range can give us a slope and intercept value which have electrochemical significance. This is because, as established by Eq. (2), the activation resistance is inversely proportional to the current. It may also be desired to model the catalyst activity and extract the time dependent electrochemical parameters namely catalyst active area, intrinsic activity and constantly estimate the activation resistance over the course of a fuel cell operation. This assumes all of the activation resistance change comes from intrinsic activity loss and no extrinsic reasons for catalyst activity reduction –namely contamination, etc. It is necessary to have the right predictors so that an appropriate model can be used. One can also continue to use higher frequency noise to generate the ohmic contribution at discrete times in a pre-meditate fashion; if no transient occurs in flow, temperature occurs. The scope of this paper is to monitor impedance to use the value to further estimate the flow rates and hence act upon to reduce the parasitic loss or to ramp up the blower.

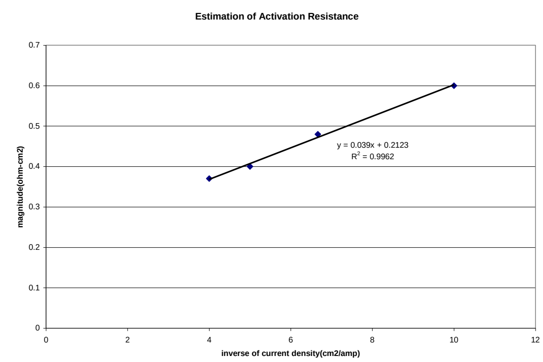

FIGURE 9. ESTIMATION OF ACTIVATION RESISTANCE USING IMPEDANCE MEASUREMENTS AT 3HZ.

3.5 Estimation vs. Measured Air Flow Rates

Figure 10 displays the measured air flow and the estimated air flow rates using measured impedance at 0.1Hz and Eq. (4). Experimental data is at 100% humidity for both cathode and anode. The inlet reactants and coolant are at 55C. The operating point was at 0.4A/cm^2 with hydrogen flow fixed and the air flow varying. The estimated flow rates were within 3.5% of the actual measured flow rates, well within the range of the stated accuracy of the flow meter itself.

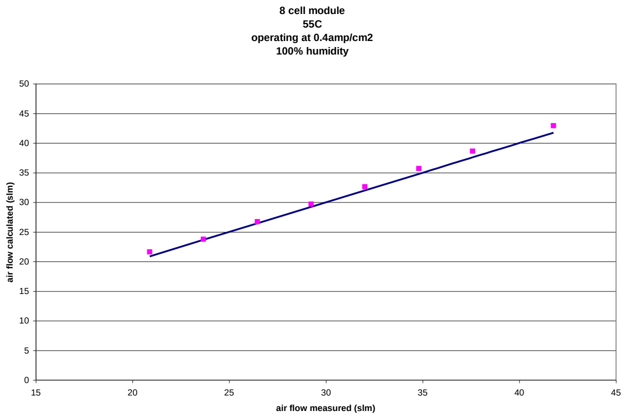

FIGURE 10. ESTIMATED AIR FLOW RATE VS. MEASURED AIR FLOW RATE. ERROR IS WITHIN 3.5%.

4. CONCLUSION

This paper provided a new technique to estimate the air flow rate using impedance measurements based on theoretical and empirical data. The estimated flow can be used in addition to stack health parameters to assess the need for dithering around a set point. This can be to minimize parasitic losses to increase the net system power.

It is clear from Fig. 4 that the impedance changes in discrete steps when the flow is changed. In contrast, the DC voltage does not show variations indicating more information is available from impedance measurements. For our 8-cell stack module, the impedance change due to flow rates can be seen at low frequencies of 3Hz at higher current densities and at lower current densities, where there is little mass transfer effect, the 3Hz will not distinguish between flows. Using 0.1Hz allows distinction at all operating current densities. It is necessary to subtract the effects due to ohmic and activation before arriving at a conclusion on the need for reacting to higher impedance. The ability to determine the current state in impedance can be use to determine if an action of increasing flow or decreasing flow may be desired. Air flow rates may be directly used to watch out on system behaviors, but such usage of flow meters are expensive and need to be calibrated once in a while to make sure of accuracy. This paper gives a first level indicator to an issue that can be immediately followed by a wide-set of meaningful actions. This provides an expected value model that necessitates constant update based on the level of hydration and also activation resistance. Future studies should include the temperature effects on impedance measurements.

ACKNOWLEDGMENTS

The work of the first and third authors is supported in part by the National Science Foundation under Grant No. ECCS 0238268.

REFERENCES

[1] Springer, T.E., Zawodzinski, T.A., Wilson, M.S., and Gottesfeld, S., 1996. "Characterization of Polymer Electrolyte Fuel Cells Using AC Impedance Spectroscopy*". J. Electrochem. Soc*., 143, pp. 587-599.

[2] Yuan, X., Sun, J., Blanco, M., Wang, H., Zhang, J., and Wilkinson, D., 2006. "AC Impedance Diagnosis of a 500W PEM Fuel Cell Stack Part I: Stack Impedance". *J. Power Sources*, 161, pp. 920-928.

[3] Makharia, R., Mathias, M., and Baker. D.,2005. "Measurement of Catalyst Layer electrolyte Resistance in PEFCs Using Electrochemical Impedance Spectroscopy". *J. Electrochem. Soc.*, 152, pp. A970-A977.

[4] Merida, W., Harrington, D.A., Le Canut, J.M., and McLean, G., 2006. "Characterisation of Proton Exchange Membrane Fuel Cell (PEMFC) Failures via Electrochemical Impedance Spectroscopy". *J. Power Sources*, 161, pp. 264-274.

[5] Gasda, M., Misiewicz, M., Prescott, G., and Meredith, J., US Patent 7099787 8/29/2006.

[6] Springer, T.E., Wilson, M.S., and Gotttesfeld, S., 1993. "Modeling and Experimental Diagnostics in Polymer Electrolyte Fuel Cells*". J. Electrochem. Soc*. 140, pp. 3513 – 3525.

[7] Pukrushpan, J., Stefanopoulou, A., and Peng, H., 2004. "Control of Fuel Cell Breathing". *IEEE Control Sys Mag*., April, pp. 30-46.

[8] St-Pierre, J., Wetton, B., Kim, G. -S., and Promislow, K.,2007. "Limiting Current Operation of Protron Exchange Membrane Fuel Cells". *J electrochem. Soc.*, 154, pp. B186-B193.